

The effect of anhydrous composition on water solubility in granitic melts

HARALD BEHRENS AND NICOLE JANTOS

Institut für Mineralogie, Universität Hannover, Welfengarten 1, D-30167 Hannover, Germany

ABSTRACT

The effect of anhydrous composition on the solubility of water in granitic melts was investigated experimentally at 800 °C and pressures from 50 to 500 MPa. Starting materials were ten natural obsidians from various localities worldwide and one re-melted leucogranite from the Himalayas.

Most of the experiments were performed in externally heated pressure vessels using Ni-NiO to buffer f_{O_2} . All samples were quenched isobarically after reaction for 120–336 h. Water contents of the resulting glasses were determined by Karl-Fischer titration.

The solubility data indicate that Na/K ratio and normative Qz content have only a minor effect on water solubility, whereas the (MCLNK-A)/O parameter, defined as $100 \cdot (2Mg + 2Ca + Li + Na + K - Al) / \text{total oxygen}$, has a major effect. A parabolic law expressed as the mole fraction of H₂O in the melt on a one-oxygen mole basis is proposed to describe the compositional dependence of water solubility in the range 50–200 MPa:

$$X_{H_2O} = X_{H_2O}^0 \cdot (1 + 0.05 \cdot \{[(MCLNK-A)/O] - 0.5\}^2)$$

Minimum mole fractions of water in the melt ($X_{H_2O}^0$) are 0.0521 at 50 MPa, 0.0757 at 100 MPa, and 0.1069 at 200 MPa. The equation fits water solubility data for granitic and phonolitic melts at 100 MPa and 200 MPa to within $\pm 4\%$ relative. The effects of anhydrous composition on water solubility are much more pronounced at 500 MPa than at lower pressures. Thus, the following expression was derived to represent the effects of anhydrous melt composition on water solubility at 500 MPa:

$$X_{H_2O} = 0.1681 \cdot (1 + 0.13 \cdot \{[(MCLNK-A)/O] - 0.5\}^2).$$

INTRODUCTION

Dissolved water has a profound influence on the chemical and physical properties of granitic melts. The addition of a small amount of water to a dry granitic melt decreases the solidus and liquidus temperatures by several hundred degrees (e.g., Tuttle and Bowen 1958), decreases the viscosity of the melt by several orders of magnitude (e.g., Shaw 1972; Dingwell et al. 1996; Schulze et al. 1996), and accelerates not only the diffusivity of melt components, but also the kinetics of crystal dissolution and growth in the melt (Chekmir and Epel'baum 1991; Watson 1994). Therefore, reliable water solubility data are required to model accurately the kinetic and thermodynamic properties of hydrous melts and to predict correctly the behavior of natural magmas. Over the past 25 years, numerous quantitative models have been developed for natural magmas in general, and/or for granitic magmas in particular (Burnham 1979; Nicholls 1980; Silver and Stolper 1985; Papale 1997; Moore et al. 1998; Yamashita 1999; Zhang 1999). All of these formulations predict the pressure and temperature dependence of water solubility. However, they often do not account for the effect of anhydrous melt composition, and all of them are ad-

versely affected by an insufficient quantity of data, and by errors in the experimental determinations of water solubility. Published H₂O solubility data for melts of granitic composition are widely scattered, and systematic discrepancies are observed between results obtained in different laboratories (Kadik et al. 1972; Khitarov and Kadik 1973; Shaw 1974; Silver et al. 1990; Blank et al. 1993; Moore et al. 1998; Yamashita 1999). As discussed by Holtz et al. (1992, 1995) and Zhang (1999), imprecision in the data is mainly due to difficulties in the experimental and analytical techniques used to measure water solubility.

For the present study, we applied experimental and analytical procedures that were successfully tested in previous investigations of H₂O solubility in feldspathic and quartzfeldspathic melts (Behrens 1995; Holtz et al. 1992, 1995). Solid starting materials for the experiments were ten natural obsidians and one re-melted leucogranite, which cover a wide range of anhydrous composition. The Fe contents of these materials were low (<5 wt% Fe₂O₃) and they contained only minor amounts of microlites (<2 vol%). The aim of the present work was to determine the chemical parameters that control H₂O solubility in natural granitic melts. Studies on simple synthetic granitic analogs, such as albitic or haplogranitic melts, have shown systematic dependencies of H₂O solubility on melt composition.

* E-mail: h.behrens@mineralogie.uni-hannover.de

For the haplogranite (Qz-Ab-Or) system, it was found that water solubility increases with the Na/K ratio of the melt but decreases with the normative Qz component (Holtz et al. 1992, 1995, 1999). In both Na aluminosilicate and haplogranite melts, a minimum in H₂O solubility as a function of alkali/Al ratio was observed for nearly subaluminous compositions (Na + K = Al) (Behrens 1995; Dingwell et al. 1997). Moreover, it has been demonstrated that F, B, and/or P increase water solubility in haplogranitic melts (Holtz et al. 1993). Natural granitic melts have more complex compositions, and variations in water solubility observed for simple synthetic analogs may be obscured by intricate interactions among the numerous components in these liquids. Thus, a comparison of results from natural and simple synthetic compositions may elucidate the mechanisms of water dissolution in silicate melts.

STARTING MATERIALS

Compositions and sources of the starting materials are summarized in Table 1. Detailed descriptions of the microtextures and origins of some of the obsidians are given elsewhere (AI: Harris 1983; MAC: Pichavant et al. 1987; EDF, LGB, BL: Stevenson et al. 1995). In addition to natural obsidians, a leucogranitic glass was produced by heating a rock powder for 8 h in a platinum crucible at 1600 °C. After three cycles of grinding and re-melting, a crystal-free and chemically homogeneous glass containing some air bubbles was obtained.

All of the natural obsidians contain minor amounts (<2 vol%) of microlites. Fine-grained magnetite was observed in each of the Fe-rich glasses, and might also be present as submicroscopic particles in the Fe-poor glasses, because Fe oxides readily crystallize from silicate melts during cooling.

Other minerals were identified during electron probe microanalysis of some of the samples (e.g., amphibole in BL, biotite in OT, alkali feldspars in NSL), but they were not characterized in detail. The homogeneity and composition of the glasses was determined by electron probe microanalysis using a CAMECA CAMEBAX instrument operated at an accelerating voltage of 15 kV and a beam current of 18 nA, with a beam diameter of 25 µm. The detected Fe₂O₃ corresponds to the bulk content of the obsidian because it was impossible to avoid magnetite completely in the measurement spot. Our microprobe analyses are in good agreement with published analyses of obsidians and leucogranite from the same locality (AI: Harris 1983; EDF, LGB, BL: Stevenson et al. 1995, MAC: Pichavant et al. 1987, Stevenson et al. 1995, GB: Scaillet et al. 1995). In general, the TiO₂, MnO, and MgO contents of the starting materials are low. The obsidian from Iceland (IL) has a relatively high CaO content of 1.68 wt%. The CIPW normative Qz contents vary between 24 wt% (AI) and 38 wt% (BL). The peralkaline obsidian NSL from New Zealand has the lowest Al₂O₃ content (10.05 wt%), but the highest Fe₂O₃ content (4.77 wt%) of the selected obsidians. The peraluminous Macusani glass differs from the other glasses in that it has very high F, Li, B, and P contents. Pichavant et al. (1987) reported F (1.3–1.4 wt%), Li₂O (0.74–0.80 wt%), B₂O₃ (0.4–0.6 wt%), and P₂O₅ (0.40–0.55 wt%) contents for Macusani glasses appearing as pebbles in a tuff matrix, and suggested they formed from residual liquids produced during fractional crystallization of the tuffs.

EXPERIMENTAL PROCEDURES

Tabular pieces of glass (2 × 2 × 5 mm) were sealed with doubly distilled water in gold tubes. The amount of water added

TABLE 1. Compositions and sources of starting materials

	EDF Armenia, Erivan Dry Fountain	LGB USA, Little Glass Butte	BL New Zealand, Ben Lommond	AI Ascension Islands	GB Himalaya, Gangotri	NSL New Zealand, *	LP Italy, Lipari Islands	IL Iceland, Robben- rücken	OT Turkey, Trabazon	QV Argentina, Quironcolo	MAC Peru, Macusani
	wt% of oxide components										
SiO ₂	77.04	77.22	77.76	72.79	74.7	75.45	75.07	75.89	76.01	75.97	72.26
TiO ₂	0.11	0.09	0.16	0.20	0.09	0.19	0.06	0.24	0.12	0.10	0.04
Al ₂ O ₃	12.76	12.95	12.30	12.49	15.2	10.05	12.77	12.09	13.42	14.12	15.83
Fe ₂ O ₃ †	0.76	0.97	1.38	3.76	0.82	4.77	1.68	3.78	0.83	0.71	0.68
MnO	0.07	0.04	0.04	0.17	0.05	0.12	0.07	0.13	0.05	0.09	0.06
MgO	0.08	0.10	0.16	0.02	0.11	0.00	0.04	0.08	0.09	0.09	0.02
CaO	0.58	0.88	1.15	0.41	0.56	0.17	0.72	1.68	0.87	0.40	0.22
Na ₂ O	4.07	3.91	3.83	5.58	4.50	5.27	4.02	4.26	4.02	3.87	4.14
K ₂ O	4.79	4.44	3.63	4.65	4.28	4.56	5.34	2.78	5.04	4.60	3.66
F	<0.03	<0.03	<0.03	0.14	0.11	<0.03	<0.03	0.06	<0.03	0.29	1.33
-O‡	–	–	–	-0.06	-0.05	–	–	–	–	-0.12	-0.56
Total	100.26	100.60	100.41	100.15	100.38	100.58	99.77	100.96	100.45	100.12	97.68 §
M(g/mol)	32.48	32.44	32.33	33.37	32.68	33.09	32.77	32.73	32.61	32.81	34.16
(MCLNK-A)/O0.52	0.63	0.92	1.09	-0.19	1.36	0.79	1.42	0.72	-0.28	-0.55	
	CIPW normative concentrations										
Qz	33.4	34.7	38.0	24.4	30.2	34.1	28.9	34.5	30.9	34.3	33.1
Or	28.4	26.2	21.4	27.5	25.3	26.9	31.6	16.4	29.8	27.2	21.6
Ab	34.6	33.1	32.4	38.4	38.1	26.3	34.0	36.1	34.0	32.7	35.0

Notes: Molar mass *M* of the anhydrous glass is calculated on one-oxygen mole basis. Calculation of the compositional parameter (MCLNK-A)/O is described in the text. (MCLNK-A)/O values >0 and <0 indicate peralkaline and peraluminous melt compositions, respectively.

* Details of the source locality are unknown.

† All iron is given as Fe₂O₃.

‡ Equivalent wt% of oxygen, for which fluorine is incorporated in the melt (2 F⁻ ↔ O²⁻).

§ Value << 100.0 in the case of the MAC composition is due to components of the glass (H₂O, Li₂O, B₂O₃, P₂O₅) which are not measured by microprobe (see Pichavant et al. 1987).

was slightly higher than the expected solubility value. A large excess of water was avoided to minimize dissolution of melt components in the fluid and precipitation of hydrous quench phases. The sealed capsules were tested for possible leakage by checking for weight loss after drying in an oven at 110 °C for at least 1 h.

Experiments were carried out in Tuttle-type externally heated pressure vessels (EHPV) at 800 °C and pressures from 50 to 500 MPa. Typically, four samples were reacted in each experiment. Water was used as the pressure medium. During the experiment, temperature was recorded continuously using a K-type thermocouple located in a bore hole of the autoclave close to the sample. The temperature at sample positions was determined in a separate run using three thermocouples. Temperature gradients were always less than 3 °C/cm, and therefore the measured values during the experiments are believed to be accurate to ± 10 °C.

The run procedure was as follows. The EHPV was open to the pressure line during heating. The final pressure was adjusted after reaching experimental temperature, and the autoclave was then isolated from the pressure line during the experiment. Strain-gauge manometers were used to measure pressure several times during each experiment. The accuracy of each pressure determination is believed to be ± 2 MPa. Oxygen fugacity was controlled in most of the experiments using a powdered mixture of Ni and NiO placed in the autoclave next to the sample capsules. At the end of the experiment, the autoclave was reconnected to the pressure line and then quenched isobarically to room temperature in a stream of compressed air. Measured initial cooling rates were ~ 3 °C/s.

ANALYTICAL PROCEDURES

No attempt was made to measure the mass of free water in the reacted samples by weight loss after piercing and heating the capsule, due to the anticipated loss of water from the hydrated glasses as they were dried. In most cases, a free fluid phase was observed after opening the capsule, or its presence was indicated by dimples on the surface of the quenched glasses (Burnham and Jahns 1962). In the other experiments, the presence of excess water was deduced from mass-balance calculations.

Water contents of the quenched glasses were measured by Karl-Fischer titration (KFT). A detailed description of this technique is given elsewhere (Behrens 1995; Holtz et al. 1995; Behrens et al. 1996). Briefly, the glasses were thermally dehydrated and the released water was measured by coulometric titration. The glasses were analyzed as single pieces or coarsely crushed powder. Typically ~ 0.10 wt% water remained in the glasses after titration (Behrens 1995). The measured water contents were corrected for this residual water.

The homogeneity of water distribution in the run products was determined by near-infrared spectroscopy using the H₂O combination mode at 5200 cm⁻¹ and the OH combination mode at 4500 cm⁻¹. Measurements were performed on doubly polished glass plates ~ 0.5 mm thick using an IR microscope (type A590) attached to a FTIR spectrometer (Bruker IFS88). No attempt was made to use IR spectroscopy for quantitative water determinations because the molar absorption coefficients of the combination bands can vary significantly with anhydrous

composition (Silver et al. 1990; Behrens et al. 1996), and they are not known with sufficient accuracy for the anhydrous compositions and ranges of water contents of our run products.

RESULTS AND DISCUSSIONS

Description of run products

Experimental data acquired in this study are summarized in Table 2. All run products were bubble-free. Microprobe analysis indicated the presence of feldspar in several of the low-pressure run products. Iron-oxide phases were found in all IL and LP samples, and also might be present in other Fe-rich glasses as submicroscopic particles. Relatively large amounts of crystals (>2 vol%) were present only in two samples (BL and IL) reacted at 50 MPa. The IL samples contain both feldspar and titanomagnetite, and the total amount of crystals is estimated to be about 2 vol% from analysis of backscattered electron images. The 50 MPa BL sample contains ~ 10 vol% pyroxene, feldspar, and amphibole. As reported by Stevenson et al. (1995), the unreacted glass contains clinopyroxene, orthopyroxene, and plagioclase.

IR spectroscopy indicates a homogeneous distribution of water within the run products. The total water content of each sample was determined by bulk analysis and, therefore, the solubility of water in the melts is underestimated when one or more crystalline phases are present. In general, crystalline phases were distributed non-uniformly in the run products, being preferentially located close to the capsule walls. Estimation of volume fractions of crystalline phases (Table 2) using an optical microscope or backscattered electron images was difficult, and we believe errors may be as large as $\pm 50\%$. For samples containing only minor crystals (all run products except the two 50 MPa IL and BL samples), no correction to the measured solubility was applied. The resulting error in water solubility is believed to be $<1\%$ relative, much smaller than the estimated error for KFT (Table 2). Water solubility for the highly crystallized BL and IL samples was corrected by subtracting a roughly estimated fraction of crystals (2 wt% for IL and 10 wt% for BL) from the sample weight used for KFT, assuming that H₂O is present exclusively in the glass.

Water solubility

The pressure dependence of water solubility in three granitic melts is illustrated in Figure 1. As observed for other silicate melts (see McMillan and Holloway 1987; McMillan 1994; Holtz et al. 1995), water solubility varies with the square root of pressure at low pressure, and converts to a quasilinear dependence on P at intermediate pressures. At higher pressure (>500 MPa), H₂O solubility is expected to increase sharply as critical conditions are approached (Paillat et al. 1992). Projected onto a Qz-Or-Ab diagram, our solubility data do not show a systematic trend (Fig. 2). Water solubility data for haplogranitic compositions AOQ and HPG 8 obtained by (Holtz et al. 1992, 1995) are close to the values for the granitic melts. However, a systematic correlation with the Qz content or the Ab/Or ratio, which has been established for the haplogranite system, is not evident for the granitic melts. This implies that other chemical parameters have a more pronounced effect on H₂O solubility in granitic melts.

TABLE 2. Experimental data for granitic melts formed at 800 °C

Sample	H ₂ O added (wt%)	Pressure (MPa)	Time (h)	Density (g/L)	C _{H₂O} KFT (wt%)†	X _{H₂O} ‡	Crystalline phases §
EDF	21.3	500	144	2219	9.94(15)	0.1661(26)	
	10.1	200	192	2263	6.26(17)	0.1075(31)	
	8.0	100	264	2273	4.27(17)	0.0745(33)	
	6.5	50	336	2323	2.83(10)	0.0499(27)	fsp (<1 vol%)
LGB	20.9	500	144	2216	10.11(12)	0.1686(21)	
	10.1	200	192	2259	6.21(12)	0.1066(23)	
	8.0	100	264	2282	4.26(17)	0.0742(33)	
	6.1	50	336	2291	2.72(10)	0.0480(26)	fsp (<1vol%)
BL	21.3	500	144	2198	10.28(17)	0.1708(29)	
	9.8	200	192	2255	6.21(17)	0.1063(31)	
	8.6	100	264	2278	4.35(11)	0.0756(24)	
	6.3	50	336	2297	2.75(12)	0.0484(29)	fsp, py, amph (total ca. 10 vol%)
AI	20.4	500	144	2235	10.69(11)	0.1821(20)	
	9.7	200	192	2306	6.41(17)	0.1130(32)	
	8.2	100	264	2328	4.51(13)	0.0808(28)	
	6.0	50	336	2372	2.83(13)	0.0514(31)	
GB	20.5	500	144	2218	10.86(16)	0.1811(28)	
	10.0	200	192	2246	6.26(11)	0.1081(22)	
	8.4	100	264	2284	4.31(14)	0.0756(29)	fsp (<1 vol%)
	6.4	50	336	2309	3.22(11)	0.0570(30)	fsp (<1 vol%)
NSL	21.3	500	144	2226	10.93(10)	0.1847(18)	
	9.7	200	192	2295	6.55(09)	0.1146(19)	
	11.0	200	192	2309	6.43(13)	0.1126(25)	
	10.3	200*	120	–	6.31(12)	0.1106(24)	
	8.4	100	264	2320	4.51(15)	0.0802(21)	
LP	6.3	50	336	2322	3.22(14)	0.0579(34)	
	10.2	200	192	2251	6.15(10)	0.1067(20)	
	IL	500	144	2197	10.75(10)	0.1801(18)	Ti-mgt (<1vol%)
IL	10.1	200	192	2312	6.07(14)	0.1054(27)	Ti-mgt (<1vol%)
	8.0	100	264	2317	4.34(12)	0.0764(26)	Ti-mgt, fsp (total < 1 vol%)
	6.4	50	336	2314	2.76(11)	0.0492(28)	Ti-mgt, fsp (total ca. 2 vol%)
	OT	200	192	2250	6.14(16)	0.1060(30)	
QV	21.4	500	144	2202	10.54(13)	0.1769(23)	
	10.3	200	192	2247	6.22(16)	0.1080(30)	
	8.6	100	264	2263	4.43(13)	0.0780(28)	
	6.5	50	336	2292	3.27(10)/3.18(16)	0.0574(29)	
MAC	10.0	200	192	2235	7.23(11)	0.1289(23)	

Notes: Estimated uncertainties for pressure, temperature and density are, respectively, ± 2 MPa, ± 10 °C and $\pm 1\%$ relative.

* Oxygen fugacity buffered by Cu + Cu₂O. The oxygen fugacities of all other samples were buffered by Ni + NiO.

† Water content of glasses were determined by bulk measurements using Karl-Fischer titration. Numbers in parentheses are estimated errors for KFT determinations of water contents (wt%), and refer to the last decimal places of the listed values.

‡ Mole fractions of dissolved water were calculated on a one-oxygen mole basis. Data for BL and IL at 50 MPa were corrected for the estimated volume fraction of crystals. Estimated uncertainties for X_{H₂O} account for possible errors in the measurements of pressure, temperature, water content, and volume fraction of crystals.

§ Crystalline phases identified by electron microprobe: alkali feldspar (fsp), pyroxene (py), titanomagnetite (Ti-mgt), amphibole (amph).

The ratio of non-bridging O atoms to tetrahedral cations (NBO/T) has often been used as a chemical parameter to describe compositional variations in silicate melts. However, NBO/T is only applicable to depolymerized melts in which the concentrations of alkali and alkaline-earth elements exceeds those required to charge-compensate trivalent, tetrahedrally coordinated cations such as Al³⁺. If the concentration of alkali and alkaline earth elements is insufficient to compensate the charge due to trivalent cations, Al³⁺ becomes a network modifier. The proportions of network-forming and network-modifying Al³⁺ in silicate melts are not well known, and probably depend on bulk composition. Therefore, characterization of non-bridging O atoms, as well as quantification of tetrahedrally coordinated (network-forming) cations, is ambiguous in Al-rich melts.

Another complication is the oxidation state of Fe in the melts at the *P*, *T*, and *f*_{O₂} conditions of our experiments. Empirical models (Sack et al. 1980; Kress and Carmichael 1991) are based mainly on 1 atm data for dry melts obtained at temperatures >1000 °C

and, therefore, they may not yield reliable Fe²⁺/Fe³⁺ ratios for hydrous melts formed at temperatures below 900 °C. Differences between calculated and measured redox states of Fe as large as one order of magnitude were observed for iron partitioning between plagioclase and hydrous tonalitic melts at temperatures 750–850 °C (Wilke and Behrens 1999).

To avoid uncertainties in quantifying the oxidation state of Fe in granitic melts, we developed the following anhydrous-melt parameter that does not depend on Fe²⁺/Fe³⁺ ratio:

$$(\text{MCLNK-A})/\text{O} = 100 \cdot (2 \text{ Mg} + 2 \text{ Ca} + \text{Li} + \text{Na} + \text{K} - \text{Al})/\text{O} \quad (1)$$

(concentrations of atoms in mol/g). For peralkaline compositions, the value of [(MCLNK-A)/O > 0] corresponds to the mole percentage of non-bridging oxygen atoms divided by total oxygen. For peraluminous melts, the parameter [(MCLNK-A)/O < 0] has no physical meaning. The compositions of the studied melts (Table 1) vary from (MCLNK-A)/O = –0.55 (peraluminous

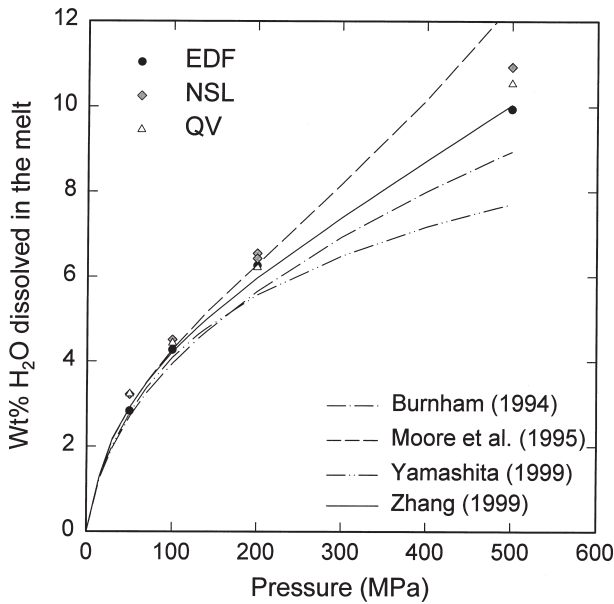


FIGURE 1. Pressure dependence of water solubility in nearly subaluminous (EDF), peralkaline (NSL), and peraluminous (QV) granitic melts at 800 °C. Water solubilities for subaluminous melts are calculated from the models developed by Burnham (1994), Moore et al. (1995), Yamashita (1999), and Zhang (1999).

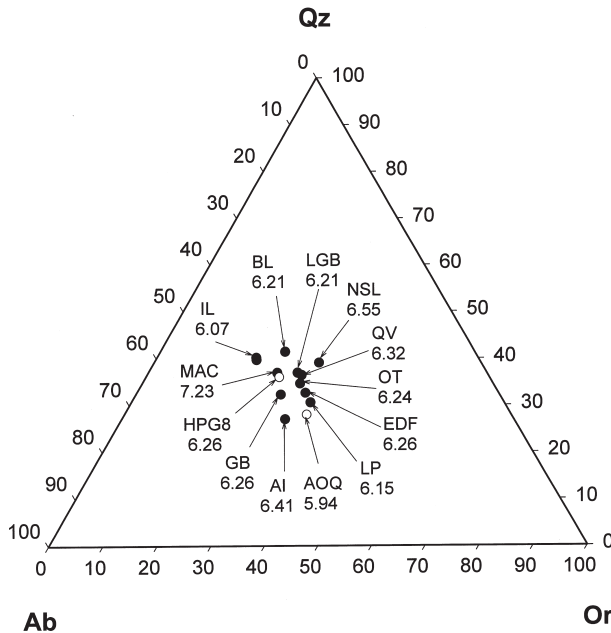


FIGURE 2. CIPW normative Qz-Or-Ab compositions (in wt%) of starting glasses, and corresponding measured water solubilities (in wt%) for 800 °C, 200 MPa. Data for haplogranitic compositions AOQ ($Qz_{28}Or_{34}Ab_{38}$) and HPG8 ($Qz_{36}Or_{25}Ab_{39}$) from Holtz et al. (1992) are shown for comparison.

melts) to $(MCLNK-A)/O = +1.36$ (peralkaline melts).

Water solubility has a minimum close to the subaluminous composition, and increases as melt composition becomes either peralkaline or peraluminous. At 100 MPa, H_2O solubili-

ties are 6% higher for the peralkaline NSL melt [$(MCLNK-A)/O = +1.36$] and 4% higher for the peraluminous QV melt [$(MCLNK-A)/O = -0.28$], compared with the slightly peralkaline EDF composition [$(MCLNK-A)/O = 0.52$]. The compositional effect seems to be more pronounced at 500 MPa, with H_2O solubilities being 10% higher for the NSL composition and 6% higher for the QV melt, compared with the EDF composition. An outlier in the 500 MPa trend is the solubility of water in the IL sample, which is relatively high for a nearly subaluminous composition. This result may indicate additional compositional effects that are not accounted for by the $(MCLNK-A)/O$ parameter. However, it is noteworthy that at lower pressures the measured water solubilities for the IL composition lie along the trend of the other data. Finally, considering the trend defined by the other granitic melts, the MAC melt has a relatively high water solubility. A possible explanation for this deviation is that the MAC composition contains abundant F, B, and Li, which are known to increase H_2O solubility (Holtz et al. 1993).

Fitting the dependence of H_2O solubility on $(MCLNK-A)/O$

At 50–200 MPa, the compositional dependence of water solubility, expressed as mole fraction of the H_2O component on a one-oxygen mole basis (X_{H_2O}), can be described by a simple parabolic law. Fitting all data (except those for the MAC composition), a minimum of water solubility was calculated for a slightly peralkaline composition close to $(MCLNK-A)/O = 0.5$. This contrasts with haplogranitic and albitic compositions for which minimum solubilities of water occur in stoichiometric [$(MCLNK-A) = 0$] or slightly peraluminous compositions (Dingwell et al. 1997; Behrens 1995). However, in the case of granitic melts, the exact position of the minimum is not well constrained by the experimental data, and the quality of the fit (expressed as r^2) decreases only slightly if the minimum is fixed at $(MCLNK-A)/O = 0$. Thus, the data for granitic melts are consistent with a minimum water solubility being close to the subaluminous composition.

The (unconstrained) form of the equation derived to represent the data for 50–200 MPa is:

$$X_{H_2O} = X_{H_2O}^0 \cdot (1 + 0.05 \cdot \{[(MCLNK-A)/O] - 0.5\}^2) \quad (2)$$

Calculated minimum mole fractions of water in the melt ($X_{H_2O}^0$) are 0.0521 at 50 MPa, 0.0757 at 100 MPa, and 0.1069 at 200 MPa. For 100 and 200 MPa, Equation 2 fits both the data listed in Table 2 and results for phonolitic melts (Carroll and Blank 1997; Moore et al. 1998) within 4% relative. Experimental temperatures were slightly higher in the studies of Carroll and Blank (850 °C) and Moore et al. (900 °C) than in the present study (800 °C), however, as the temperature dependence of H_2O solubility typically is small [a decrease of 0.16 wt% per 100 °C was found by Holtz et al. (1995) for haplogranitic melts at 100 and 200 MPa], it is likely that using the phonolitic data without corrections does not significantly affect the results. For 50 MPa, differences between the solubilities listed in Table 2 and those calculated from Equation 2 are small (<0.25 wt%). However, values for phonolitic melts (Carroll and Blank 1997) are significantly smaller than those indicated by the trend of the results for granitic compositions. In addition, a relatively small

variation of H₂O solubility with (MCLNK-A)/O is inferred from the 50 MPa data for haplogranitic melts having an excess of alkalis (Na, K, Rb, Cs) relative to Al (Dingwell et al. 1997). Thus, for 50 MPa, extrapolating Equation 2 beyond (MCLNK-A)/O = 2 may produce large errors.

Fitting the 500 MPa data (neglecting the aberrant value obtained for composition IL) to the parabolic equation yields

$$X_{\text{H}_2\text{O}} = 0.1681 \cdot (1 + 0.13 \cdot \{[(\text{MCLNK-A})/\text{O}] - 0.5\}^2) \quad (3)$$

Due to scatter in the data, the fit parameters have large uncertainties. Therefore, Equation 3 is only semi-quantitative in representing the compositional dependence of H₂O solubility in granitic melts. Nevertheless, the relatively large variation of H₂O solubility with (MCLNK-A)/O is consistent with results for haplogranitic melts at the same pressure (Dingwell et al. 1997).

A weakness of our approach to modeling the compositional dependence of water solubility is that the concentration and oxidation state of Fe are not considered. This may be the reason why some of the solubility data lie off the general trends shown in Figure 3 (e.g., melt IL at 500 MPa). If Fe²⁺ behaves as an MCLNK-type cation and Fe³⁺ has the properties of an A-

type cation, it would be expected that oxidation of the melt would reduce the (MCLNK-A)/O value. To test this possibility, we performed one experiment with the Fe-rich NSL composition at oxidizing conditions. In this particular run, the double-capsule technique described by Eugster and Wones (1962) was applied. The sample was sealed in an inner Ag₇₅Pd₂₅ capsule and then loaded into an outer Au capsule, along with the buffer assemblage (Cu, Cu₂O + H₂O). Because hydrogen permeates rapidly through Ag₇₅Pd₂₅, osmotic equilibrium was reached at 800 °C within a few minutes (Chou 1986). Although Au is much less permeable to hydrogen, redox equilibration is expected to be achieved rapidly (within one day) in our other solubility experiments because only small masses of heterovalent cations were present in the samples. A detailed discussion of the kinetics of redox equilibration at the experimental conditions is given by Wilke and Behrens (1999). The H₂O solubility was slightly lower (6.31 wt%) in the melt equilibrated with the Cu/Cu₂O buffer than in those equilibrated with the Ni/NiO buffer (two reacted samples containing 6.43 and 6.55 wt% H₂O). Although the difference is within experimental uncertainty, the trend is nevertheless in accordance with the observed dependence of H₂O solubility on (MCLNK-A)/O. Thus, we infer that a more accurate modeling of water solubility in magmas is possible only by considering the speciation of Fe in the melt.

Comparison with computational models

In Figure 1, H₂O solubility data for selected granitic melts are compared with values predicted by four models. The model of Burnham (1994) systematically underestimates the solubility of water in the nearly subaluminous EDF melt over the entire range of pressure with deviations being particularly large at high pressure (10% at 500 MPa). At pressures where they nominally apply, the models of Moore et al. (1998) and Yamashita (1999) are in fairly good agreement with our data for the EDF composition (Moore et al. performed experiments at pressures up to 300 MPa, Yamashita at pressures up to 100 MPa). However, extrapolating these models to higher pressures (which is not recommended by the authors) produces large discrepancies. For 500 MPa, the model of Moore et al. (1998) overestimates H₂O solubility by 25% and that of Yamashita (1999) underestimates H₂O solubility by 23%. The best overall agreement between calculated and experimentally determined solubilities is obtained using the model of Zhang (1999), which is based on H₂O solubility data for a haplogranitic melt studied by Holtz et al. (1992, 1995). The maximum deviation of calculated values from our experimentally determined values, observed for the EDF composition, is -0.31 wt% (4.6% relative) at 200 MPa.

The models developed by Zhang (1999) and Yamashita (1999) do not account for the effects of anhydrous composition. Moore et al. (1998) linked the compositional variation of H₂O solubility in magmas to the concentrations of Na₂O, Al₂O₃, and total FeO. Their empirical model provides reliable water solubilities for subaluminous granitic melts at pressures up to 300 MPa, but fails to predict the experimentally determined trends of water solubility for peraluminous and peralkaline compositions. In addition, the calculated water solubility for

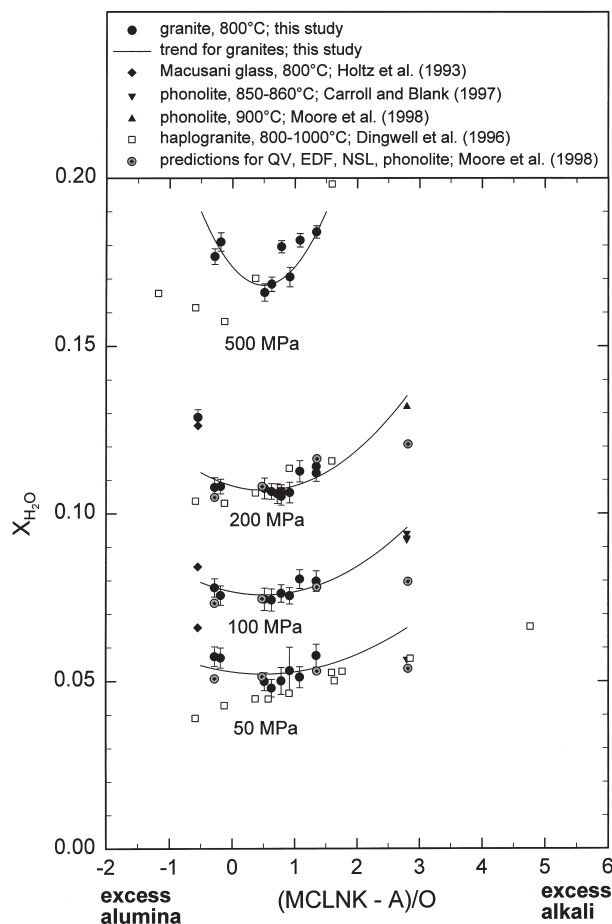


FIGURE 3. Compositional dependence of water solubility in granitic melts expressed as mole fraction of H₂O component on a one-oxygen mole basis.

phonolitic melts at 200 MPa is ~1 wt% lower than their own experimental determination of that solubility, despite the fact that data for phonolitic melts were used in the calibration of their model. Further, the coefficient for Al_2O_3 has a negative value and, consequently, the model predicts that water solubility decreases as anhydrous composition changes from subaluminous to peraluminous (increasing Al_2O_3 content for a constant alkali content). This trend is inconsistent not only with previous data for haplogranitic melts obtained by Dingwell et al. (1997) and Linnen et al. (1996), but also with the observation (this study) that water solubility is higher in QV melt than in EDF melt. These apparent inaccuracies in the model of Moore et al. (1998) can be attributed to the use of a relatively small database to derive the pressure, temperature, and compositional dependence of H_2O solubility for a large range of melts. An extended data set, and consideration of additional chemical parameters [e.g., the (MCLNK-A)/O parameter proposed in this paper], is required to improve the empirical model.

ACKNOWLEDGMENTS

This work, supported by the DAAD-NSF cooperation program was completed while H. Behrens was a visiting scientist at the University of Michigan, Ann Arbor (U.S.A.). The authors thank F. Holtz, A. Withers, and Y. Zhang for helpful comments during preparation of the manuscript. Constructive and thorough reviews by H. Nekvasil, P. Ihinger, and J. Blencoe are also gratefully acknowledged.

REFERENCES CITED

- Behrens, H. (1995) Determination of water solubilities in high-viscosity melts: an experimental study of $\text{NaAl}_3\text{Si}_3\text{O}_8$ and $\text{KAl}_3\text{Si}_3\text{O}_8$ melts. *European Journal of Mineralogy*, 7, 905–920.
- Behrens, H., Romano, C., Nowak, M., Holtz, F., and Dingwell, D.B. (1996) Near-infrared spectroscopic determination of water species in glasses of the system $\text{MAl}_3\text{Si}_3\text{O}_8$ (M = Li, Na, K): an interlaboratory study. *Chemical Geology*, 128, 41–63.
- Blank, J.G., Stolper, E.M., and Carroll, M.R. (1993) Solubility of carbon dioxide and water in rhyolitic melt at 850 °C and 750 bars. *Earth and Planetary Science Letters*, 119, 27–36.
- Burnham, C.W. (1979) The importance of volatile constituents. In H.S. Yoder, Ed., *The evolution of the igneous rocks*, p. 439–482. Princeton University Press, Princeton, New Jersey.
- (1994) Development of the Burnham model for prediction of H_2O solubility in magmas. In M.R. Carroll and J.R. Holloway, Eds., *Volatiles in Magmas*, 30, 123–129. Reviews in Mineralogy, Mineralogical Society of America, Washington, D.C.
- Burnham, C.W. and Jahns, R.H. (1962) A method of determining the solubility of water in silicate melts. *American Journal of Science*, 260, 721–745.
- Carroll, M.R. and Blank, J.G. (1997) The solubility of H_2O in phonolitic melts. *American Mineralogist*, 82, 549–556.
- Chekmir, A.S. and Epel'baum, M.B. (1991) Diffusion in magmatic melts: New study. In L.L. Perchuk and I. Kushiro, Eds., *Physical Chemistry of Magmas*. Advance in Physical Geochemistry, 9, 99–119.
- Chou, I.M. (1986) Permeability of precious metals to hydrogen at 2 kb pressure and elevated temperatures. *American Journal of Science*, 286, 638–658.
- Dingwell, D.B., Romano, C., and Hess, K.U. (1996) The effect of water on the viscosity of a haplogranitic melt under *P-T-X* conditions relevant to silicic volcanism. *Contributions to Mineralogy and Petrology*, 124, 19–28.
- Dingwell, D.B., Holtz, F., and Behrens, H. (1997) The solubility of H_2O in peralkaline and peraluminous granitic melts. *American Mineralogist*, 82, 434–437.
- Eugster, H.P. and Wones, D.R. (1962) Stability relations of the ferruginous biotite, annite. *Journal of Petrology*, 3, 82–125.
- Harris, C. (1983) The petrology of lavas and associated plutonic inclusions of Ascension Island. *Journal of Petrology*, 24, 424–470.
- Holtz, F., Behrens, H., Dingwell, D.B., and Tailor, R.P. (1992) Water solubility in melts of haplogranitic composition at 2 kbar. *Chemical Geology*, 96, 289–302.
- Holtz, F., Dingwell, D.B., and Behrens, H. (1993) Effects of F, B_2O_3 and P_2O_5 on the solubility of water in haplogranite melts compared to natural silicate melts. *Contributions to Mineralogy and Petrology* 113, 492–501.
- Holtz, F., Behrens, H., Dingwell, D.B., and Johannes, W. (1995) H_2O solubility in haplogranitic melts: Compositional, pressure, and temperature dependence. *American Mineralogist*, 80, 94–108.
- Holtz, F., Roux, J., Behrens, H., and Pichavant, M. (1999) Water solubility in SiO_2 - $\text{NaAlSi}_3\text{O}_8$ melts. *American Mineralogist*, 85, 682–686.
- Kadik, A.A., Lukanin, O.A., Lebedev, Y.B., and Korovushkina, E.Y. (1972) Solubility of H_2O and CO_2 in granite and basalt melts at high pressures. *Geochemistry International*, 1041–1050.
- Khitarov, N.I. and Kadik, A.A. (1973) Water and carbon dioxide in magmatic melts and peculiarities of the melting process. *Contributions to Mineralogy and Petrology*, 41, 205–215.
- Kress, V.C. and Carmichael, I.S.E. (1991) The compressibility of silicate liquids containing Fe_2O_3 and the effect of composition, temperature, oxygen fugacity and pressure on their redox states. *Contributions to Mineralogy and Petrology*, 108, 82–92.
- Linnen, R.L., Pichavant, M., and Holtz, F. (1996) The combined effects of f_{O_2} and melt composition on the SnO_2 solubility and tin diffusivity in haplogranitic melts. *Geochemica et Cosmochimica Acta*, 60, 4965–4976.
- McMillan, P. (1994) Water solubility and speciation models. In M.R. Carroll and J.R. Holloway, Eds., *Volatiles in Magmas*, 30, 131–156. Reviews in Mineralogy, Mineralogical Society of America, Washington, D.C.
- McMillan, P. and Holloway, J. (1987) Water solubility in aluminosilicate melts. *Contributions to Mineralogy and Petrology*, 97, 320–332.
- Moore, G., Vennemann, T., and Carmichael, I.S.E. (1998) An empirical model for the solubility of H_2O in magmas to 3 kilobars. *American Mineralogist*, 83, 36–42.
- Nicholls, J. (1980) A simple model for estimating the solubility of H_2O in Magmas. *Contributions to Mineralogy and Petrology*, 74, 211–220.
- Paillat, O., Elphick, S.C., and Brown, W.L. (1992) The solubility of water in $\text{NaAl}_3\text{Si}_3\text{O}_8$ melts: a re-examination of Ab- H_2O phase relationships and critical behaviour at high pressure. *Contributions to Mineralogy and Petrology*, 112, 490–500.
- Papale, P. (1997) Thermodynamic modeling of the solubility of H_2O and CO_2 in silicate liquids. *Contributions to Mineralogy and Petrology*, 126, 237–251.
- Pichavant, M., Herrera, J.V., Boulmier, S., Briquieu, L., Joron, J.-L., Juteau, M., Marin, L., Michard, A., Sheppard, S.M.F., Treuil, M., and Vernet, M. (1987). The Macusani glasses, SE Peru: evidence of chemical fractionation in peraluminous magmas. In B.O. Mysen, Ed., *Magmatic Processes: Physicochemical Principles*, p. 359–374. The Geochemical Society, Special Publications 1, Washington, D.C.
- Sack, R.O., Carmichael, I.S.E., Rivers, M., and Ghiorso, M.S. (1980) Ferric-ferrous equilibria in natural silicate liquids at 1 bar. *Contributions to Mineralogy and Petrology*, 75, 369–376.
- Scaillet, B., Pichavant, M., and Roux, J. (1995) Experimental crystallization of leucogranite magmas. *Journal of Petrology* 36, 663–705.
- Schulze, F., Behrens, H., Holtz, F., Roux, J., and Johannes, W. (1996) The influence of water on the viscosity of a haplogranitic melt. *American Mineralogist*, 81, 1155–1165.
- Shaw, H.R. (1972) Viscosities of magmatic liquids: An empirical method of prediction. *American Journal of Science*, 272, 870–893.
- (1974) Diffusion of H_2O in granitic liquids: Part I. Experimental data; Part II. Mass transfer in magma chambers. In A.W. Hofmann, B.J. Giletti, H.S. Yoder, and R.A. Yund, Eds., *Geochemical Transport and Kinetics*, p. 139–170. Carnegie Institution Publication, Washington, D.C.
- Silver, L.A. and Stolper, E. (1985) A thermodynamic model for hydrous silicate melts. *Journal of Geology*, 93, 161–177.
- Silver, L.A., Ihinger P.D., and Stolper E. (1990) The influence of bulk composition on the speciation of water in silicate glasses. *Contributions to Mineralogy and Petrology*, 104, 142–162.
- Stevenson, R.J., Dingwell, D.B., Webb, S.L., and Bagdassarov, N.S. (1995) The equivalence of enthalpy and shear stress relaxation in rhyolitic obsidians and quantification of the liquid-glass transition in volcanic processes. *Journal of Volcanology and Geothermal Research*, 68, 297–306.
- Tuttle, O.F. and Bowen, N.L. (1958) Origin of granite in the light of experimental studies in the system $\text{NaAlSi}_3\text{O}_8$ - KAlSi_3O_8 - SiO_2 - H_2O . *Geological Society of America, Memoirs*, 74, 1–153.
- Watson, E.B. (1994) Diffusion in volatile-bearing Magmas. In M.R. Carroll and J.R. Holloway, Eds., *Volatiles in Magmas*, 30, 371–411. Reviews in Mineralogy, Mineralogical Society of America, Washington, D.C.
- Wilke, M. and Behrens, H. (1999) The dependence of partitioning of Fe and Eu between plagioclase and hydrous tonalitic melts on oxygen fugacity. *Contributions to Mineralogy and Petrology*, 137, 102–104.
- Yamashita, S. (1999) Experimental study of the effect of temperature on water solubility in natural rhyolitic melt to 100 MPa. *Journal of Petrology*, 40, 1497–1507.
- Zhang, Y. (1999) H_2O in rhyolitic glasses and melts: Measurement, speciation, solubility, and diffusion. *Reviews Geophysics*, 37, 493–516.

MANUSCRIPT RECEIVED AUGUST 10, 1999

MANUSCRIPT ACCEPTED SEPTEMBER 14, 2000

PAPER HANDLED BY JAMES G. BLENCOE